Deletion of the Ω-Loop in the Active Site of Staphylococcal Nuclease. 2. Effects on Protein Structure and Dynamics†

Donna M. Baldisseri and Dennis A. Torchia*
Bone Research Branch, National Institute of Dental Research, National Institutes of Health, Bethesda, Maryland 20892
Leslie B. Poole and John A. Gerlt
Department of Chemistry and Biochemistry, University of Maryland, College Park, Maryland 20742
Received November 14, 1990; Revised Manuscript Received February 8, 1991

ABSTRACT: It has been shown (Poole et al., 1991) that deletion of residues 44–49 from the sequence of staphylococcal nuclease (E43 SNase) results in an enzyme (E43 ΔSNase) that is significantly more active than D43 SNase, an enzyme that differs from the wild-type enzyme by deletion of a single methylene group. In addition, both E43 ΔSNase and D43 ΔSNase are significantly more stable than their respective parent enzymes. Herein we use high-resolution 2D and 3D NMR spectroscopy to characterize the solution conformations of the four enzymes in order to better understand their differences in stability and activity. The backbone assignments of E43 SNase were extended to the three mutant proteins (uniformly ^{15}N-enriched) by using 2D HSQC, 3D HOHAHA–HMQC, and 3D NOESY–HMQC spectra. The NOE patterns observed for E43 and D43 SNase in solution are consistent with the crystal structures of these proteins. The NOESY data further show that the intact and deleted proteins have essentially the same structures except that (a) the disordered Ω-loops in the intact proteins are replaced by tight type II′ turns, formed by residues 43-50-51-52, in the deleted proteins and (b) the orientation of the D43 side chain in crystalline D43 SNase differs from that found for D43 ΔSNase in solution. Except for regions neighboring the Ω-loops, the intact and deleted proteins show nearly identical amide ^{15}N and ^{1}H chemical shifts. In contrast, there are widespread, small and similar, chemical shift differences (a) between E43 SNase and D43 SNase and (b) between E43 ΔSNase and D43 ΔSNase. This observation indicates that deletion of the E43 γ-methylene group causes small, widespread, and similar changes in the structures of E43 SNase and E43 ΔSNase.

In the previous paper (Poole et al., 1991) it is shown that deletion of residues 44–49 from the Ω-loop[1] at the active site of E43 SNase yields an active enzyme, E43 ΔSNase, having V_{max} ca. 2% that of E43 SNase. Thus the activity of E43 ΔSNase, in which six residues have been deleted from the wild-type sequence, is greater than that of D43 SNase, which differs from the wild-type enzyme by deletion of a single methylene group. The deletion of the six residues significantly enhances the stability of both E43 ΔSNase and D43 ΔSNase relative to the enzymes containing the intact Ω-loops.

In order to better understand the physical basis for the changes in enzyme activity and stability that accompany the mutations, we have used 2D and 3D NMR spectroscopy to compare the solution structures of the wild-type and mutant nucleases. Although highly refined crystal structures are available for E43 (Loll & Lattman, 1989) and D43 SNase (Loll & Lattman, 1990) complexed with pdTp and Ca^{2+}, a comparison of these crystal structures with NOE distance constraints, especially for residues at the active site, is of interest because Loll and Lattman (1989) have noted that the active-site structure observed in the crystalline enzyme may be influenced by interactions of pdTp with Lys residues in an adjacent protein molecule in the crystal lattice.

In contrast with E43 and D43 SNase, crystal structures are not available for the deleted proteins. Although modeling studies indicate that residues 43-50-51-52 can form a tight turn in the deleted proteins, while the wild-type protein structure is retained elsewhere (Poole et al., 1991), the actual structure of these residues must be determined by experiment. High-resolution NMR techniques can provide detailed structural information about proteins having M_r ca. 20 kDa, provided that isotopic enrichment is employed (Torchia et al., 1989; Wang et al., 1990a,b; Driscoll et al., 1990a,b; McIntosh et al., 1990). Uniform enrichment with ^{15}N is particularly attractive because it is inexpensive and because chemical shift assignments and NOE distance constraints are obtained from a single sample by 2D and 3D heteronuclear NMR experiments (Marion et al., 1989a,b; Zuiderweg & Fesik, 1989; Driscoll et al., 1990a,b). Herein we show that the backbone amide assignments of E43 SNase (Torchia et al., 1989; Wang et al., 1990a,b) are readily extended to the mutant SNase samples by using 2D HSQC (Bax et al., 1990), 3D HOHAHA–HMQC (Marion et al., 1989b), and 3D NOESY–HMQC (Marion et al., 1989a,b) spectra. The NOE data provide information about the structure of residues 43-50-51-52 in the deleted proteins, and the NOE and chemical shift data are used to compare the structures, particularly at the active sites, of the four proteins in solution. In addition, the observed NOE patterns and the crystalline interproton distances are used to

† This research was supported by the AIDS Targeted Antiviral Program of the Office of the Director of the National Institutes of Health (D.A.T.), by NIH GM-34573 (J.A.G.), and by NIH NRSA GM-13211 (L.B.P.).

[1] Abbreviations: Ω-loop, residues E43–E52 of wild-type staphylococcal nuclease; E43 SNase, wild-type staphylococcal nuclease; D43 SNase, staphylococcal nuclease in which E43 is replaced by D43; E43 ΔSNase and D43 ΔSNase, E43 SNase and D43 SNase, respectively, with residues 44–49 deleted [for further discussion of nomenclature see Poole et al. (1991)]; NMR, nuclear magnetic resonance; pdTp, thymidine 3′,5′-bisphosphate; HSQC, heteronuclear single-quantum spectroscopy; HMQC, heteronuclear multiple-quantum spectroscopy; HOHAHA, homonuclear Hartmann–Hahn spectroscopy; NOESY, nuclear Overhauser effect spectroscopy; [^{2}H]TSP, sodium [2,2,3,3-$^2H_4$]-3-(trimethylsilyl)-propionate.

0006-2960/91/0430-3628$02.50/0

compare the E43 and D43 SNase solution structures with the crystal structures.

Materials and Methods

Samples of SNase were fully ^{15}N-labeled by growing N4830 *Escherichia coli* in supplemented M9 media (Hibler et al., 1987) containing [^{15}N]ammonium chloride, [^{15}N]His, [^{15}N]Ile, and [^{15}N]Val as described previously (Torchia et al., 1989). The proteins were purified as described by Poole et al. (1991). As a consequence of the construction of the SNase plasmid, the SNase produced by the *E. coli* has a heptapeptide appended to the N-terminus. These seven residues as well as the first five residues in the wild-type sequence are flexible and disordered and have no known effect upon the structure and function of the enzyme (Calderon et al., 1985). For these reasons, we did not make a strong effort to assign these residues and their assignments are not included in Table IS.

NMR spectra were recorded on SNase solutions having the following composition: NaCl, 100 mM; SNase, 1.5–1.8 mM; pdTp, 5 mM; $CaCl_2$, 10 mM; borate buffer, 50 mM. The pH meter readings of the SNase solutions were in the range 6.35–6.45.

All spectra were recorded at 37 °C on a modified Bruker AM500 spectrometer. The 2D HSQC spectra were obtained by using the Overbodenhausen (Bax et al., 1990) pulse scheme. Water suppression was achieved by using a weak (ca. 25 Hz) decoupling field applied during the acquisition delay, the proton decoupling during t_1 was achieved by applying a 180° pulse during the middle of the ^{15}N evolution. WALTZ-16 (Shaka et al., 1983) modulation was used to decouple ^{15}N nuclei from protons during t_2. Lorentzian-to-Gaussian transformation was used for processing the data in both the t_1 and t_2 dimensions. The t_1 and t_2 acquisition times were 200 and 128 ms, respectively, and the final digital resolution was 4 Hz (F_1) and 8 Hz (F_2). The total number of t_1 increments was 1024, and 16 transients were acquired per t_1 value. The 3D spectra were recorded by using the NOESY–HMQC and HOHAHA–HMQC pulse schemes (Marion et al. 1989a,b; Driscoll et al., 1990a,b). The NOESY–HMQC sequence used herein is

^1H PS $90°_{\phi 1}$ t_1 $90°_x$ τ_m $90°_x$ $180°_x$ Acq(t3)

^{15}N decouple $\delta\, 90°_\psi\, t_2\, 90°_x\, \delta$ decouple

with the following phase cycling: $\phi_1 = 4(x, -x)$, $\psi = 2(x)$, $2(-x)$, $2(x)$, $2(-x)$, and Acq = $(x, -x)$, $2(-x, x)$, $(x, -x)$. The 3D HOHAHA–HMQC sequence used here is

^1H PS $90°_{\phi 1}$ t_1 TP τ_m TP $90°_x$ τ $90°_{\phi 2}$ $180°_x$ Acq(t3)

^{15}N decouple $\delta\, 90°_\psi\, t_2\, 90°_{\phi 3}\, \delta$ decouple

with the following phase cycling: $\phi_1 = 4(x, -x)$, $\phi_2 = 4(x)4(y)$, $\phi_3 = 2(x, x, -x, -x)$, and Acq = $(x, -x, -x, x, -y, y, y, -y)$. In both experiments quadrature detection in F_1 and F_2 is achieved by the TPPI-States method (Marion et al., 1989c). Each time t_1 is incremented, ϕ_1 and the receiver phase are incremented by 180°. Each time t_2 is incremented, ψ and the receiver phase are incremented by 180°. Data obtained for $\phi_1 = (x, y)$ and $\psi = (x, y)$ are stored separately and processed as complex data. The 90° pulse widths were 25 μs, ^1H; 65 μs, high-power ^{15}N; and 240 μs, low-power ^{15}N for decoupling. In both experiments weak (20–25 Hz) ^1H DANTE presaturation (PS) was applied for ca. 1 s to suppress the water resonance, and the delay δ was set to 4.5 ms, slightly less than $1/2J_{NH}$. In the NOESY experiments water suppression was also applied during the mixing period, τ_m = 100 ms. In the 3D HOHAHA–HMQC experiments, the trim pulse (TP) was 2 ms, the mix period τ_m = 36 ms, and fixed delay $\tau = \tau_m/2$ = 18 ms. Mixing was accomplished by using a DIPSI-2 sequence (Shaka et al., 1988), and the fixed delay was used to remove rotating frame NOE effects. Decoupling in t_1 and t_3 was achieved by using WALTZ-16 modulation. Proton chemical shifts are relative to the water signal, at 4.66 ppm from [^{2}-H]TSP at 37 °C, and ^{15}N chemical shifts are relative to liquid NH_3 (Ikura et al., 1990).

For both types of 3D experiments the F_3, F_2, and F_1 spectral widths were 8065, 1163, and 5000 Hz, respectively, when the carrier was placed at the water resonance, 4.66 ppm. In each experiment 128 complex t_1, 32 complex t_2, and 1024 real t_3 data points were sampled with acquisition times of 25.6 (t_1), 27.5 (t_2), and 64 (t_3) ms, respectively. The 3D NOESY–HMQC spectra of E43 and D43 SNase were recorded with the RF carrier set at 8.66 ppm, F_3 = 4000 Hz, and 512 real points were acquired in F_3. Under these conditions the data size is half that required when the carrier is set at the water resonance, 4.66 ppm; however, artifacts sometimes appear at 8.66 ppm in F_3. Hence, the NOESY–HMQC spectra of E43 ΔSNase and D43 ΔSNase were acquired with the carrier set at 4.66 ppm, as were all HOHAHA–HMQC spectra. In the case of the NOESY–HMQC experiments on E43 and D43 SNase, 16 transients were acquired for each (t_1, t_2) increment and the relaxation delay was 0.8 s, resulting in a total accumulation time of 66 h. For all other 3D experiments, eight transients per (t_1, t_2) were acquired with a 1.1-s relaxation delay, resulting in a total accumulation time of 44 h.

The 2D NMR spectra were processed on a Bruker ASPECT 1000 data station and on a SUN 4 computer. The 3D NMR spectra were processed on a SUN 4 computer using a combination of in-house and commercially available software (New Methods Research Inc., Syracuse, NY) as described previously (Kay et al., 1989a). The residual solvent component in the free induction decay signal was removed by using a time-domain convolution difference procedure (Marion et al., 1989d) with K = 8. Zero filling (once in t_2 and t_3 and twice in t_1) and discarding the upfield half of the spectrum in F_3 resulted in a final absorptive spectrum of 512 × 64 × 512 data points. Sine squared bell and sine bell weighting functions (60° shifted) were applied in the F_1 and F_3 dimensions, respectively. A 60° doubly shifted sine bell function (Kay et al., 1989a) was applied in F_2. The digital resolution in each 3D spectrum is 9.8, 18.1, and 7.9 Hz/point in F_1, F_2, and F_3, respectively.

Results

Approximately 95% of the backbone amide signals of E43 SNase have been assigned (Torchia et al., 1989, Wang et al., 1990a,b), and herein these assignments have been extended, Table 1S, to include all amides in the folded portion of the protein (i.e., the portion of SNase that includes residues 6–143) except for E43, E57, and T44. The assignments listed in Table IS were obtained at pH 6.4, rather than at 7.4 as reported previously (Torchia et al., 1989), in order to better observe several amide protons that rapidly exchange with solvent at the higher pH. The pH 6.4 assignments were derived from three-dimensional NOESY–HMQC and HOHAHA–HMQC spectra in conjunction with the available assignments at pH 7.4. A comparison of HSQC spectra of ^{15}N-labeled E43 SNase samples at pH 6.4 and pH 7.4 showed that the amide nitrogen and proton chemical shifts of nearly all residues were the same. This observation allowed rapid assignments of the amide signals at the lower pH. The correlations observed in the two 3D spectra confirmed the assignments made by comparing the chemical shifts, and, in addition, the high sensitivity

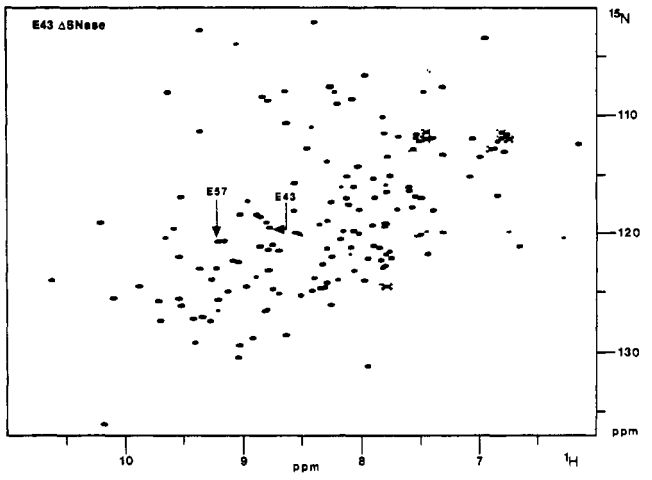

FIGURE 1: HSQC spectrum of uniformly ^{15}N-labeled E43 ΔSNase. The arrows identify the intense correlations of E43 and E57, which are absent in the corresponding spectrum of E43 SNase.

of the 3D experiments and the slower amide exchange at the lower pH allowed us to obtain assignments of all E43 SNase amides except E43, T44, and E57. We have not observed the amide signals of E43, E57, or T44 in (a) the 3D spectra of uniformly ^{15}N-labeled E43 SNase or in (b) 2D HMQC and HSQC spectra, obtained at various pH values (5.4–7.4) and temperatures (4–37 °C), of E43 SNase samples that were enriched with either [^{15}N]Glu or [^{15}N]Thr. The reason that these amide signals were not detected is discussed below.

The amide signal assignments of the mutant SNase samples were made in the following way. First an HSQC spectrum of the uniformly ^{15}N-labeled mutant protein, Figure 1, was obtained and compared with the assigned HSQC spectrum of E43 SNase. Typically a large number (ca. 50) of isolated signals that had nearly the same chemical shifts in the E43 SNase and mutant SNase samples were tentatively assigned by comparing the wild-type and mutant HSQC spectra. These assignments were then confirmed and extended to the remaining amide signals by using the extensive number of correlations observed in the 3D HOHAHA–HMQC and NOESY–HMQC spectra of the ^{15}N-labeled mutant SNase samples. The assignment procedure was facilitated by the fact that the NOESY connectivity patterns of the E43 SNase and mutant SNase samples were nearly identical.

The amide nitrogen and proton assignments obtained for the four SNase samples are summarized in Table IS. Table IS reveals that three amides of E43 SNase and nine amides of D43 SNase are not assigned, whereas all amides in the two loopless proteins, E43 ΔSNase and D43 ΔSNase, are assigned. Assignments were not obtained for some of the residues in or adjacent to the Ω-loop in the intact proteins. In contrast, all of the amides were assigned in the deleted proteins. A variety of observations have shown that the Ω-loop is disordered (Loll & Lattman, 1989, 1990) and flexible (Torchia et al., 1989; Kay et al., 1989b). Slow motion of the Ω-loop evidently results in exchange broadening in E43 and D43 SNase that makes it difficult to observe signals of residues in or near the loop. The Ω-loop of crystalline D43 SNase is more disordered than the loop of crystalline E43 SNase. The fact that fewer loop amides have been observed for D43 than for E43 SNase indicates that, in solution, the D43 SNase loop is also more disordered than the E43 SNase loop.

The differences in the ^{1}H and ^{15}N chemical shifts of E43 and D43 SNase are depicted in Figure 2, panels a and b, respectively. As expected, there are significant differences in chemical shifts of residues near the mutation site, e.g., T41, V51, and E52. More surprising are the large chemical shift differences seen elsewhere in the sequence, particularly involving residues 19–22 and 58–63.

We examined how the differences in amide chemical shifts correlated with the differences in the structures of E43 and D43 SNase. In agreement with the crystal structures (Loll & Lattman, 1989, 1990) the backbone NOE patterns observed for E43 and D43 SNase were the same except for residues in the loop region, which were not observed in D43. In the crystal structures of E43 and D43 SNase, the loops are disordered and their structures are imprecisely defined. However, the electron density maps show that the loop structures differ significantly in the two proteins (Loll & Lattman, 1989, 1990). Assuming that the loop structures of E43 and D43 SNase differ in solution as well, we rationalize the observation of chemical shift differences for residues 19–22 and 58–63, where the two proteins have the same backbone structures, by noting that the loop is close to these residues, Figure 3. Therefore, the change in loop structure is responsible for changing the chemical shift of these residues.

In addition to the large changes observed in the loop structure, small differences (ca. 0.16 Å rms) were found in the α-carbon positions of residues 7–41 and 54–141 in the crystal structures of E43 and D43 SNase (Loll & Lattman, 1989, 1990). While these differences in α-carbon positions are comparable to the estimated rms coordinate errors, a plot of the difference in C^{α} position as a function of residue number indicated that the structures of E43 and D43 were slightly different. This result is consistent with the small, widespread differences in amide chemicals shifts of E43 and D43 SNase seen in Figure 2, panels a and e.

The large changes in the conformation of the Ω-loop and the small structural changes that accompany the E43D mutation complicate the interpretation of the different activities of E43 and D43 SNase. Therefore, the observation that the deleted proteins, E43 ΔSNase and D43 ΔSNase, were considerably more stable than E43 and D43 SNase suggested that the structural differences between the loopless proteins might be confined to the mutation site, thus making differences in enzyme activity easier to interpret.

Significant differences in amide chemical shifts of E43 SNase and E43 ΔSNase, Figure 2, panels b and f, are expected and seen for residues 19–22 and 50–63, as a consequence of the deletion of loop residues 44–49. More interesting is the observation that chemical shifts elsewhere in the sequence are virtually identical for E43 SNase and E43 ΔSNase, suggesting that the deletion causes only a local change in structure. This conclusion was confirmed by comparison of the 3D NOESY–HMQC spectra of E43 SNase and E43 ΔSNase. The only significant differences in the observed backbone NOE patterns were confined to residues 43-50-51-52 and to a few residues whose amide signals were broadened by loop motion in E43 SNase. Furthermore we found that, except for residues 43-50-51-52, the NOE backbone patterns observed for E43 ΔSNase were in agreement with the interproton distances calculated from the E43 SNase X-ray coordinates. Therefore, except for residues 43-50-51-52, the backbone structures of E43 SNase and E43 ΔSNase are essentially the same.

The secondary structure of residues 43-50-51-52 was determined by comparing the NOE patterns observed in slices of the 3D NOESY-HMQC spectrum of E43 ΔSNase, Figure 4a, with the NOE patterns calculated for four types of common tight turns (Wagner et al., 1986; Wuethrich, 1986), Figure 5. On the basis of the following reasoning, residues 43-50-51-52 form a type II′ turn. A single strong d_{NN} con-

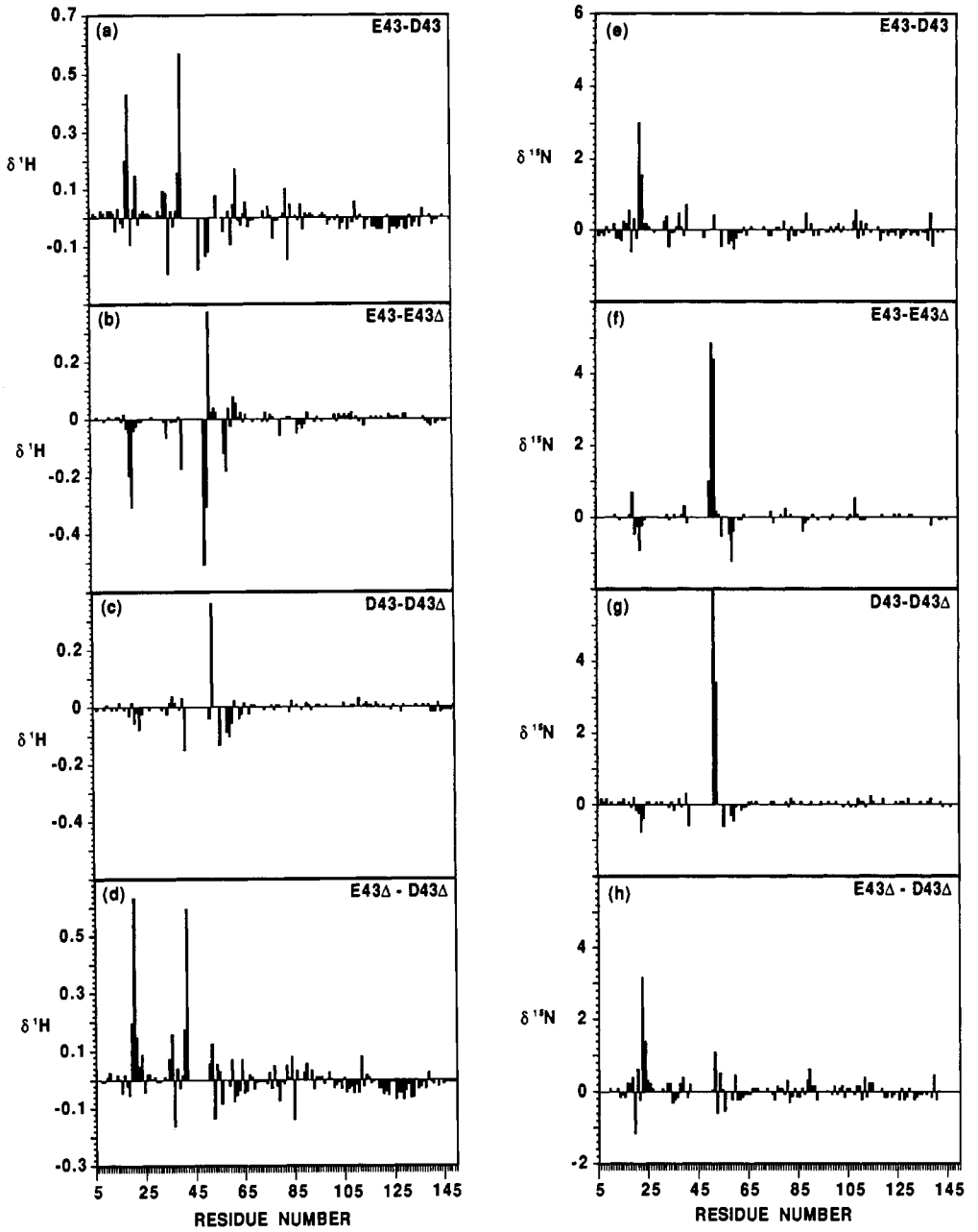

FIGURE 2: Differences in amide ^1H, left panel, and ^{15}N, right panel, chemical shifts plotted against residue number: (a,e) E43 SNase − D43 SNase; (b,f) E43 SNase − E43 ΔSNase; (c,g) D43 SNase − D43 ΔSNase; (d,h) E43 ΔSNase − D43 ΔSNase.

nectivity linking the amides of V51 and E52 is observed. According to Figure 5, this implies that the turn must be type II or II′ since two d_{NN} connectivities, $d_{NN}(50,51)$ and $d_{NN}(51,52)$, would be observed in the case of either a type I or I′ turn. Type II and II′ turns are distinguished on the basis of the intensity of the intraresidue $d_{\alpha N}(51,51)$ connectivity. According to Figure 5, this connectivity is very strong for a type II turn and weak for a type II′ turn. The weak $d_{\alpha N}(51,51)$ connectivity observed in Figure 4a established that E43 ΔSNase contained a type II′ turn. We note in passing that because one of the two G50 α-protons is close (2.2 Å) to the V51 amide proton for both the type II and the type II′ turns, the sequential $d_{\alpha N}$ (50,51) connectivity can be used to distinguish these two turn types only when the second residue in the turn has a chiral α-carbon. We also note that glycine must be the second residue in a type II′ turn if unfavorable steric contacts are to be avoided.

The amide chemical shift differences of D43 SNase and D43 ΔSNase, like those of E43 SNase and E43 ΔSNase, are limited to residues that neighbor the Ω-loop and are accounted for by the replacement of the disordered Ω-loop by a type II′ turn. The latter conclusion follows from the observation that the NOE patterns for residues 43-50-51-52 are essentially the same for E43 ΔSNase and D43 ΔSNase, Figure 4. No significant differences were observed in the D43 SNase and D43 ΔSNase NOE patterns elsewhere in the protein sequence.

We now examine the NOE patterns of the side chains of the residues that compose the SNase active site, in order to determine the extent to which the mutations affect their conformations. The crystal structures show that the active site of SNase contains side chains of D21, R35, D40, E/D43, K84, Y85, R87, Y113, and Y115. With the exception of residues E43 and D43, the NOE patterns observed for the active-site residues, Figures 6 and 1S (a) are in agreement with the interproton distances obtained from the crystal structures of E43 SNase and D43 SNase and (b) are the same, within experimental error, for all four proteins. Hence, the solution and crystalline conformations of these residues are nearly the same in E43 SNase and in D43 SNase, and the differences in the conformations of these residues in the four proteins are

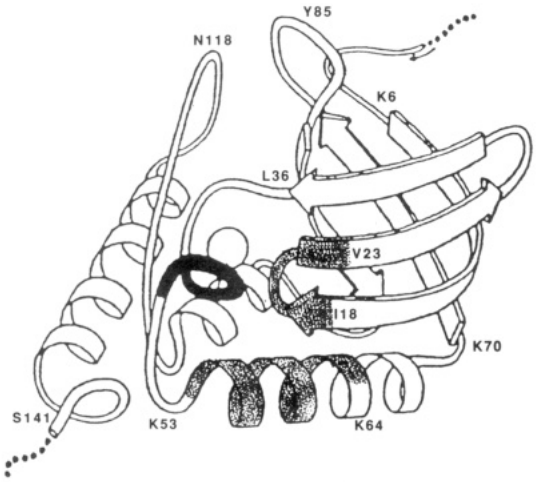

FIGURE 3: Ribbon diagram of E43 SNase (Richardson, 1981) showing the proximity of the omega loop, black segment, to residues 19–22 and 54–63, stippled segments.

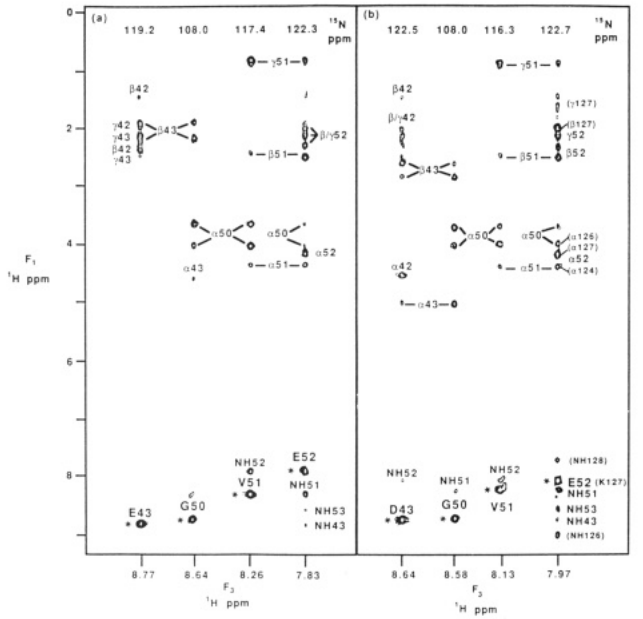

FIGURE 4: Composite of strips from the 3D NOESY-HMQC spectra of (a) E43 ΔSNase and (b) D43 ΔSNase for residues E(D)43, G50, V51, and E52. The chemical shifts of the diagonal amide proton signals (identified by an asterisk) of these residues are given on the horizontal axis. In (a) the α42 proton is at 4.66 ppm and is saturated.

very small. This latter conclusion is supported by the observation that the side chain protons have nearly the same chemical shifts in the four proteins. Particularly striking are the γ-protons of K84 that are upfield-shifted by the Y85 ring to the same positions in the four spectra, Figure 6. This observation shows that the relative positions of the K84 and Y85 side chains must be essentially the same in the four proteins.

Because the amide signals of E43 and D43 have not been observed in E43 SNase or D43 SNase, we have not been able to compare the NOESY patterns of residues 43 in these proteins with the corresponding NOESY patterns in the deleted proteins. The 3D NOESY–HMQC spectrum of D43 ΔSNase, Figure 4b, shows one strong and one weak intensity $d_{N\beta}(43,43)$ connectivity. A crystal structure is not available for D43 ΔSNase, but the D43 SNase crystal structure predicts two strong $d_{N\beta}(43,43)$ cross peaks, in disagreement with the NMR data. We cannot yet compare the E43 NOESY pattern predicted by the X-ray structure of E43 SNase with the E43 NOESY pattern observed for E43 ΔSNase in solution, because

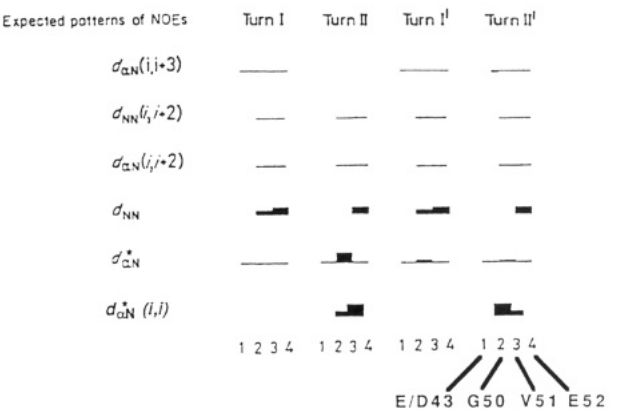

FIGURE 5: NOE patterns computed for the various tight turn types. The $d_{\alpha N}(i,i)$ patterns are shown only for residues 2 and 3 of the type II and II′ turns because these intraresidue connectivities are used to distinguish the II and II′ turn types. Where indicated by an asterisk, the turn II and II′ $d_{\alpha N}$ NOE patterns for the second glycine α-proton are obtained by interchanging the turn II and II′ glycine $d_{\alpha N}$ NOE patterns shown. The same remarks apply to the type I and I′ turn patterns.

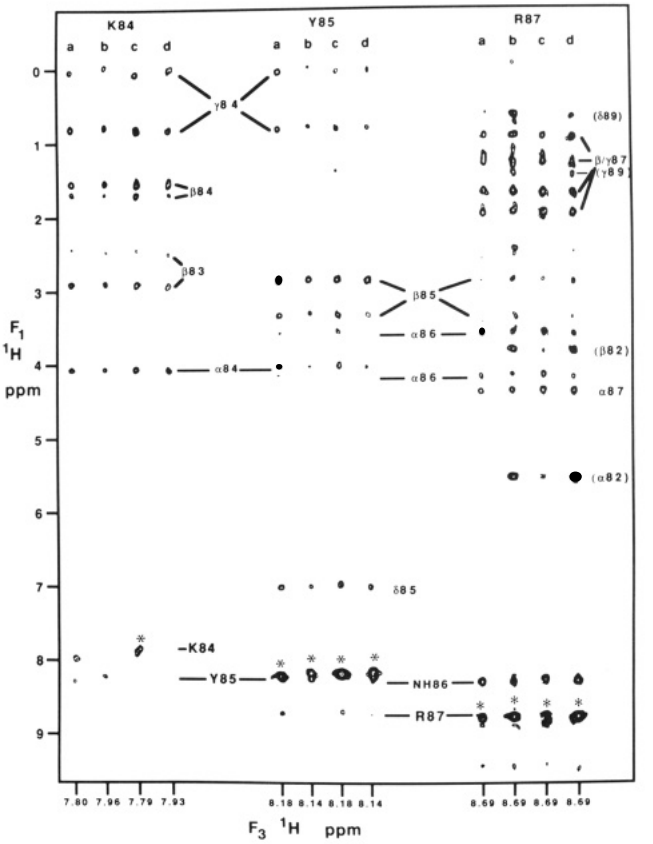

FIGURE 6: Comparison of strips of the 3D NOESY–HMQC spectra of (a) E43 SNase, (b) D43 SNase, (c) E43 ΔSNase, and (d) D43 ΔSNase for active-site residues K84, Y85, and R87. The chemical shifts of the diagonal amide protons of K84, Y85, and R87 (identified by an asterisk) are given on the horizontal axis. Due to exchange with water, the amide protons of K84 are nearly saturated. The NOE connectivities in parentheses arise from D83, whose amide ^{1}H and ^{15}N shifts nearly coincide with those of R87.

the $d_{N\beta}(43,43)$, $d_{N\gamma}(43,43)$, and $d_{\beta N}(42,43)$ cross peaks overlap, Figure 4a. We expect to overcome this problem in subsequent studies by incorporating [*ring*-$^2H_6$]Pro into SNase.

Discussion

In general, the NMR results obtained for E43 and D43 SNase samples are in agreement with observations made for the crystalline proteins. The Ω-loops in both proteins are disordered and flexible in solution, and the larger number of

missing amide signals in the case of D43 SNase is consistent with the observation that the D43 loop in the crystal is more disordered in the case of D43 than E43 SNase. The numerous small differences in amide ^{15}N and ^{1}H chemical shifts of E43 SNase and D43 SNase indicate that the E43D mutation causes a myriad of small changes in proton positions, a result that agrees with the conclusions of the X-ray work. There are significant differences between the crystal structures of E43 and D43 SNase at the active site; namely, (a) the carboxyl groups of E43 and D43 have different orientations and (b) several of the water molecules that contribute to the hydrogen-bond network at the active site of E43 SNase (including the water molecule thought to be the attacking nucleophile) are absent in the crystal structure of D43 SNase. While these structural differences in the E43 and D43 SNase active sites significantly affect activity, they do not result in significant changes in internuclear distances of protons observed in the NMR experiments. Hence, if the E43 and D43 SNase crystal structures are preserved in solution, active-site residues will exhibit the same NOE patterns in the two proteins, as observed. Furthermore, the observation that the NOE patterns of active-site residues are consistent with the X-ray structures of E43 SNase and D43 SNase is noteworthy because of the concern that interaction of pdTp with the K70 and K71 side chains, derived from an adjacent molecule in the crystal lattice, might influence the SNase crystal structure (Loll & Lattman, 1989, 1990).

The NOE data show that the deleted proteins have a type II′ turn, at residues 43-50-51-52, in place of the Ω-loop. This structural alteration may explain the greater stability of the deleted enzymes, although other explanations are possible (Poole et al., 1991). No other backbone conformational differences among the four proteins are evident in the NOESY spectra. However the observation of widespread, small amide chemical shift differences between E43 SNase and D43 SNase, and of a similar set of differences between E43 ΔSNase and D43 ΔSNase, suggests that the E43D mutation produces a similar set of small structural changes in the intact and deleted proteins. Taken together, the NMR and X-ray (Loll & Lattman, 1989, 1990) data indicate that the deletion of a single methylene moiety causes small but widespread changes in the detailed organization of SNase.

The NOESY pattern observed for the D43 side chain in D43 ΔSNase is not consistent with values of $d_{N\beta}(43,43)$ reported in the crystal structure of D43 SNase. Furthermore the orientations of the E43 and D43 side chains differ in the E43 SNase and D43 SNase crystal structures (Loll & Lattman, 1989, 1990). These results together with the other results presented herein suggest that changes in the detailed structure of the tight turn at residues 43-50-51-52 will affect the orientation of the E43 side chain but not significantly alter the conformation of residues outside the tight turn. We are currently investigating the effect of mutations of residues 50 and 51 on the activity and structure of deleted SNase. We think that it may be possible to elucidate how the conformation of E43 is related to the efficiency of E43 as a general base catalyst. The deleted proteins are attractive subjects for this study because deletion of the Ω-loop residues eliminates exchange broadening and thus allows signals of all residues to be observed.

Acknowledgments

We thank Drs. Ad Bax, Mitsuhiko Ikura, and Lewis Kay for helpful discussions of their 3D pulse sequences and data processing programs. We are grateful to Rolf Tschudin for expert technical support.

Supplementary Material Available

Table IS, listing the amide proton and nitrogen assignments of the four proteins, and Figure 1S, showing the strips of the 3D NOESY–HMQC spectra of the four proteins for active-site residues D21, R35, D40, Y113, and Y115 (4 pages). Ordering information is given on any current masthead page.

Registry No. L-Glu, 56-86-0; L-Asp, 56-84-8; staphylococcal nuclease, 9013-53-0.

References

Bax, A., Ikura, M., Kay, L. E., Torchia, D. A., & Tschudin, R. (1990) *J. Magn. Reson. 86*, 304–318.

Calderon, R. O., Stolowich, N. J., Gerlt, J. A., & Sturtevant, J. M. (1985) *Biochemistry 24*, 6044–6049.

Driscoll, P. C., Clore, G. M., Marion, D., Wingfield, P. T., & Gronenborn, A. M. (1990a) *Biochemistry 29*, 3542–3556.

Driscoll, P. C., Gronenborn, A. M., Wingfield, P. T., & Clore, G. M. (1990b) *Biochemistry 29*, 4668–4682.

Hibler, D. W., Stolowich, N. J., Reynolds, M. A., Gerlt, J. A., Wilde, J. A., & Bolton, P. H. (1987) *Biochemistry 26*, 6278–6286.

Ikura, M., Kay, L. E., & Bax, A. (1990) *Biochemistry 29*, 4659–4667.

Kay, L. E., Marion, D., & Bax, A. (1989a) *J. Magn. Reson. 83*, 72–84.

Kay, L. E., Torchia, D. A., & Bax, A. (1989b) *Biochemistry 28*, 8972–8979.

Loll, P. J., & Lattman, E. E. (1989) *Proteins: Struct., Funct., Genet. 5*, 183–201.

Loll, P. J., & Lattman, E. E. (1990) *Biochemistry 29*, 6866–6873.

Marion, D., Kay, L. E., Sparks, S. W., Torchia, D. A., & Bax, A. (1989a) *J. Am. Chem. Soc. 111*, 1515–1517.

Marion, D., Driscoll, P. C., Kay, L. E., Wingfield, P. T., Bax, A., Gronenborn, A. M., & Clore, G. M. (1989b) *Biochemistry 28*, 6150–6156.

Marion, D., Ikura, M., Tschudin, R., & Bax, A. (1989c) *J. Magn. Reson. 85*, 393–399.

Marion, D., Ikura, M., & Bax, A. (1989d) *J. Magn. Reson. 84*, 425–430.

McIntosh, L. P., Wand, A. J., Lowry, D. F., Redfield, A. G., & Dahlquist, F. W. (1990) *Biochemistry 29*, 6341–6362.

Poole, L. B., Loveys, D. A., Hale, S. P., Gerlt, J. A., Stanczyk, S. M., & Bolton, P. H. (1991) *Biochemistry* (preceding paper in this issue).

Richardson, J. S. (1981) *Adv. Protein Chem. 34*, 167–189.

Serpersu, E. H., Hibler, D. W., Gerlt, J. A., & Mildvan, A. S. (1989) *Biochemistry 28*, 1539–1548.

Shaka, A. J., Keeler, J., & Freeman, R. (1983) *J. Magn. Reson. 53*, 313–340.

Shaka, A. J., Lee, C. J., & Pines, A. (1988) *J. Magn. Reson. 77*, 274–293.

Torchia, D. A., Sparks, S. W., & Bax, A. (1989) *Biochemistry 28*, 5509–5524.

Wagner, G., Neuhaus, D., Worgotter, E., Vasak, M., Kagi, J. R. H., & Wuethrich, K. (1986) *J. Mol. Biol. 187*, 131–135.

Wang, J., LeMaster, D. M., & Markley, J. M. (1990a) *Biochemistry 29*, 88–101.

Wang, J., Hinck, A. P., Loh, S. N., & Markley, J. M. (1990b) *Biochemistry 29*, 102–113.

Wuethrich, K. (1986) *NMR of Proteins and Nucleic Acids*, Wiley, New York.

Zuiderweg, E. R. P., & Fesik, S. W. (1989) *Biochemistry 28*, 2387–2391.